

Effects of Wall Angles and Performance Prediction of Unsteady Flow through a Two Dimensional Diffuser

Mr. ESAM M. ABED
DEPT. OF MECH. ENG.
UNIVERSITY OF BABYLON
BABEL, IRAQ

Mr. RIYADH S. AL-TURHEE
DEPT. OF MECH. ENG.
UNIVERSITY OF BABYLON
BABEL, IRAQ

ALI A. AL-KAYIEM
DEPT. OF MECH. ENG.
UNIVERSITY OF BABYLON
BABEL, IRAQ

الملخص:

النواشر ثنائية الأبعاد تستخدم في العديد من التطبيقات، من هذه التطبيقات في الماكينات التوربينية بطريقة التحليل استعملت لإيجاد توزيع ضغط السكون والضغط الكلي للناشر دون الصوتي مع وجود التناظر أو ثنائية الأبعاد في المقطع المستخدم. تم استخدام المانع اللزج المضطرب الغير مستقر وتم الحل النهائي للمعادلات بطريقة العناصر المحددة. النواشر التي تم استخدامها هي ثنائية الأبعاد، مستقيمة الجدران لعدد من الزوايا و نسب مساحة الدخول والخروج قد تم بحثها نظريا بحيث لا يتكون لدينا مناطق انفصال الجريان. عامل الاضطراب عرف باستخدام نموذج الاضطراب (k-ε).

Abstract

Tow-dimensional diffusers are used for a variety of applications, such as turbo machines. An analytical procedure for computing the static and total pressure distribution subsonic diffuser with axi-symmetric or two dimensional cross-sections used. Finite element procedures for incompressible viscous fluid motion, turbulent, unsteady flow are used in this paper. The unsteady flow problem is solved by the Newton-Raphson method. Straight-walled, two-dimensional diffusers for several aspect ratio and angles were investigated theoretically for the purpose of studying the regime of no appreciable stall. Introducing the (k-ε) model to the work also used the effect of turbulence.

1. Introduction: -

The deceleration of flowing fluid, or diffusion as it is widely known, is a process of primary importance whereby some of the kinetic energy of the flowing fluid is converted into static pressure rise. Hence, fluid motion take places against an adverse pressure gradient, and unless great care is taken in the design of diffusing system. From the point of view of the fundamental of fluid motion, the study of diffusing flows is indeed very interesting. Therefore, it has attracted the attention of many investigators, and a great deal has been published on performance of various diffuser configurations, e.g., conical, annular, rectangular, radial.

There is a wealth of literature on flow through the diffuser. Many researchers presented design and analysis of the diffuser, both experimental and analytical solution. Riyadh [1], presented the mathematical model for the two-dimensional diffuser in centrifugal compressor. The flows described in this research steady state, and turbulent flow. K. Eisele, A. Öngören, P. Holbein and M.V. Casey [2], described the dedicated test rig for planar diffuser flows of different opening angles is available and has been modified to take the flow conditions such as inlet blockage and inlet turbulence level of a typical turbo-machinery diffuser into account. The flow in this diffuser was analyzed with LDA at different opening angles in the range of attached and stalled flow regimes.

The measurements show that a three-dimensional separation of the flow sets-in a corner at moderate opening angles and grows with increasing diffuser angles to a big separation zone downstream. Kai U. Ziegler¹, Heinz E. Gallus and Reinhard Niehuis [3], presented the interaction between impeller and diffuser is considered to have strong influence on the flow in highly loaded centrifugal compressors. However, the knowledge about this influence is still not satisfying. This two-part paper presents an experimental investigation of the effect of impeller-diffuser interaction on the unsteady and the time averaged flow configuration in impeller and diffuser and the performance of these components. The flat wedge vaned diffuser of the investigated stage allows an independent adjustment of diffuser vane angle and radial gap between impeller exit and diffuser vane inlet. Attention is mainly directed to the radial gap, as it determines the intensity of the impeller-diffuser interaction

The diffusing passage two dimensional diffusers considered here is show in Fig. (1). Geometry is fixed by aspect ratio, $[b/W1]$, and any two of the for dimensionless geometric parameters, $(2\theta, L/W1)$. The computational procedure taken solves the time average Navier-Stokes equation for unsteady state, incompressible and turbulent flow in two-dimensional situations. Analysis of the flow inside the diffuser was based on finite element technique, by using Galerkin method.

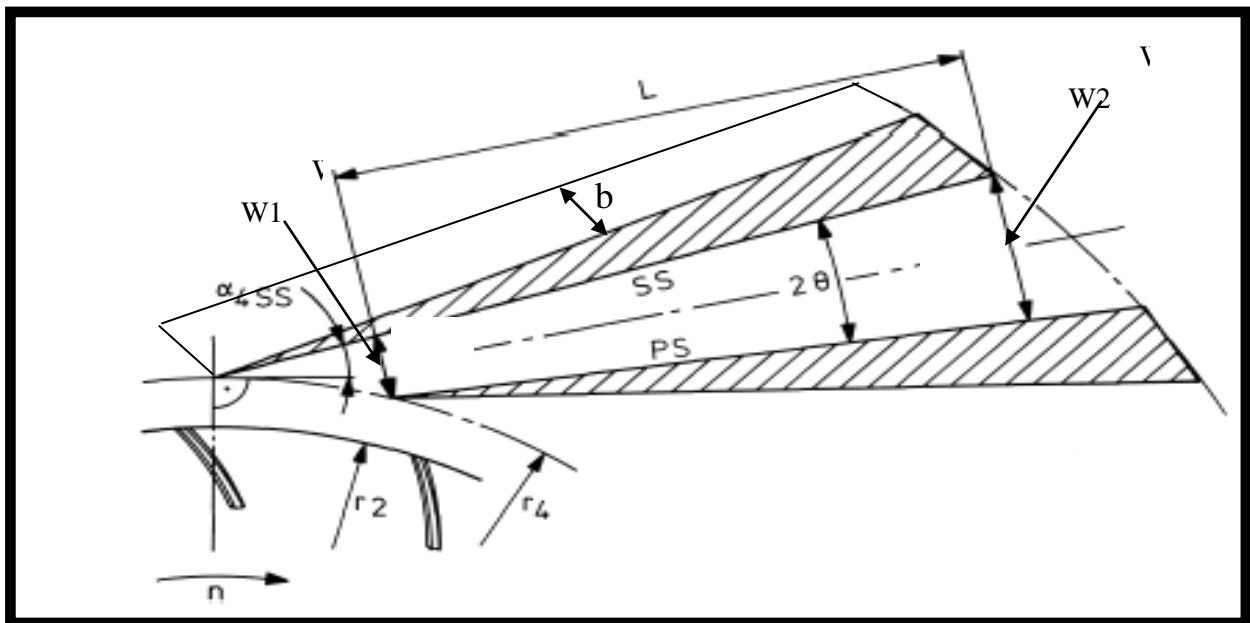


Fig. (1) Two-dimensional diffuser for centrifugal compressor.

2. Design and parameter of diffuser:-

The simple two dimensional diffuser may be described by three geometric parameters, the area ratio (AR), the divergence angle of one way (θ), and the ratio of the wall length to entry width (L/W). The parameters are illustrated in Fig. (1). But only two of the three will be independent since they are related by Ref. [4] as:

$$AR = 1 - 2 \frac{L}{W} \sin \theta \quad \dots (1)$$

It has been common practice to plot of diffuser characteristics against (2θ) and (L/W) . An alternate method would be to use $(AR-1)$ and (L/W) . Several combinations have been used in this

paper, since each has its own advantages.

The geometric of simple vaned island type diffuser system consists of a number of channels, as shown in Fig. (2). The channel can be divided into three regions, the flow region (1) is unsteady and very unsettled because of jet and wakes emanating from rotating impeller passage and these tend to mix as the flow advances towards the diffuser throat. Region (2) clearly conforms to parallel wall rectangular diffuser. In region (3), as in region (1), the flow is bounded by the diffuser blade only on one side. Hence, the mechanism of diffusion would not be the same as in the region (2), as described by Ref. [5].

Because the distance from the wall is very important, therefore takes path (1), and it's at (0.02m) distance from the wall. In this paper, it is intended to design region (2) only, in designing the diffuser, several models under line (A-A) of Fig. (3) Were taken, as illustrated by [5, 6 and 7].

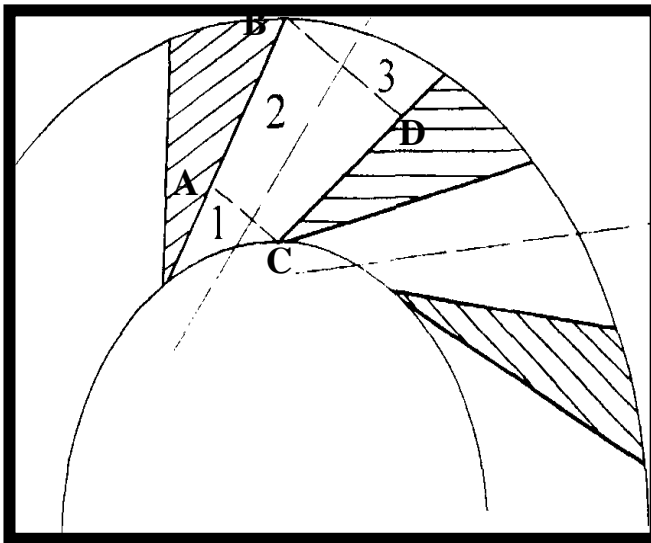


Fig. (2) Wedge type vane Island diffusers

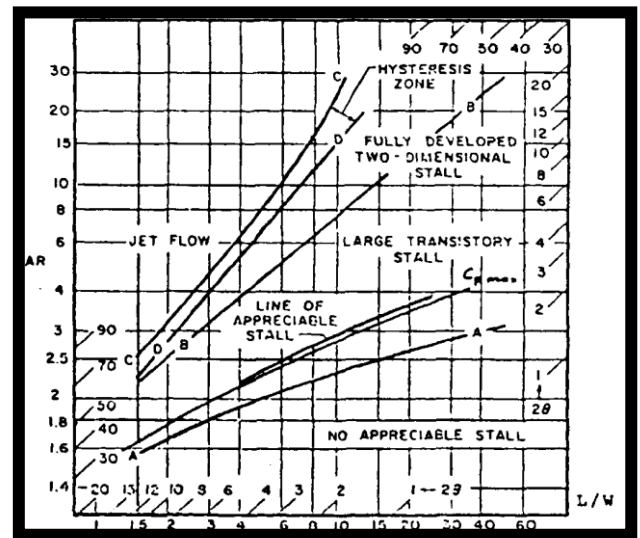


Fig. (3) Flow Regimes for two-dimension diffuser.

3. Variation Equations

The basic conservation equations are the continuity and motion which for unsteady state, take the following time averaged form in two-dimensional case [8 and 9].

•Continuity

$$u_{i,j} = 0 \quad \dots(2)$$

•motion

$$\rho \left(\frac{\partial u}{\partial t} + u_{i,j} u_j \right) - \sigma_{ij,j} = 0 \quad \dots(3)$$

Where:

$$\sigma_{ij} = (-P\delta_{ij} + 2\mu_{eff}d_{ij}) \quad \text{and} \quad d_{ij} = \frac{1}{2}(u_{i,j} + u_{j,i})$$

The well known Navier-Stokes equation can be obtained by introducing equations (σ_{ij}) and

(d_{ij}) into equation (3) and using equation (2).

$$\rho \left(\frac{\partial u}{\partial t} + u_{i,j} u_j \right) + P_i - \mu_{eff} u_{i,jj} = 0 \quad \dots (4)$$

• **Two equation turbulence modeling**

In this paper the turbulent effects are included via a k- ϵ model, which is based on the transport of two additional turbulent quantities, the turbulent kinetic energy (k) and its dissipation rate (ϵ) for high Reynolds number, with two dimensional unsteady flow. These two additional balance equations may be written in the following form, [8 and 10] as: -

$$\rho \frac{DK}{Dt} = \frac{\partial}{\partial y} \left(\frac{\mu_{eff}}{\sigma_k} \frac{\partial k}{\partial y} \right) + \mu_{eff} \left(\frac{\partial u}{\partial y} \right)^2 - \rho \epsilon \quad \dots (5)$$

$$\rho \frac{D\epsilon}{Dt} = \frac{\partial}{\partial y} \left(\frac{\mu_{eff}}{\sigma_\epsilon} \frac{\partial \epsilon}{\partial y} \right) - C_1 \frac{\epsilon}{k} \mu_{eff} \left(\frac{\partial u}{\partial y} \right)^2 - C_2 \frac{\rho \epsilon^2}{k} \quad \dots (6)$$

Where

$$\mu_{eff} = \mu_l + \mu_T \quad \text{and} \quad \mu_T = C_\mu \rho k^2 / \epsilon$$

At high Reynolds numbers, ϵ may be assumed proportional to $(\rho k^{3/2} / \ell)$ Here, σ_k , C_1 , σ_ϵ , C_2 and C_μ are the turbulence model constants, which are respectively equal to 1.0, 1.44, 1.3, 1.92 and 0.09 respectively.

• **Pressure Recovery Coefficient: -**

This is the most widely used parameter and it gives static pressure rise as a function of the inlet velocity head, i.e.;

$$C_p = \frac{P_2 - P_1}{\frac{1}{2} \rho V_t^2} \quad \dots (7)$$

4. **Finite Element Analysis**

To apply the finite element method, variation equation corresponding to equation (2) and (3) are required. They can be obtained by employing the conventional procedure called Galerkin method. Let u_i^* be the weighting function. Multiplying both side of equation (3) by u_i^* , integrating over the whole volume V and using Greens theorem, the following is obtained, [9, 11 and 12].

$$\int_V \rho \frac{\partial u_i}{\partial t} u_i^* dV = \int_V u_i^* u_{i,j} u_j dV + \int_V u_i^* \sigma_{ij,j} dV = 0 \quad \dots (8)$$

Introducing equations (σ_{ij}) and (d_{ij}) and rearranging them, the final form of the variation equation is derived.

$$\int_V \rho \frac{\partial u_i}{\partial t} u_i^* dV = \int_V \rho u_i^* u_{i,j} u_j dV - \int_V (P u_{i,j}^*) dV + \mu_{eff} \int_V u_{i,j}^* (u_{i,j} + u_{j,i}) dV = 0 \quad \dots (9)$$

As to the equation of continuity, after multiplying both sides of equation (2), by weighting

function and integrating over the whole volume \mathbf{V} , the variation equation is expressed in the following:

$$\int_{\mathbf{V}} (P^* u_{i,j}) dV = 0 \quad \dots (10)$$

Assume that the flow field to be analysis is divided into small regions called finite elements, let the interpolating equation for velocity and pressure in each finite element be expressed by the following form, [12]:

$$u_i = \Phi_{\alpha} u_{\alpha i} \quad \dots (11)$$

$$P = \Psi_{\lambda} P_{\lambda} \quad \dots (12)$$

Where Φ_{α} and Ψ_{λ} denote interpolation function or shape function for velocity and pressure respectively. ($u_{\alpha i}$) means the velocity at α th nodes of each finite element in the i th direction, and (P_{λ}) is the pressure at the λ th node. Using the finite element mesh, the flow inside diffuser has been studies.

The boundary conditions are given as follows Fig. (2).

$$u=0 \text{ and } v=0 \quad \text{for all nodes at (AB and CD).} \quad \dots (13)$$

$$u=100 \text{ and } v=0 \quad \text{for all nodes at AC.} \quad \dots (14)$$

$$P=0 \quad \text{for all nodes at BD.} \quad \dots (15)$$

For weighting function u_i^* , and P_{λ}^* , the relation that is similar to equations (11) and (12) are used as follows.

$$u_i^* = \Phi_{\alpha} u_{\alpha i}^* \quad \dots (16)$$

$$P^* = \Psi_{\lambda} P_{\lambda}^* \quad \dots (17)$$

Introducing equations (11), (12), (16) and (17) into equations (9) and (10), the following finite element equations can be obtained for motion and continuity as:

$$M_{\alpha i \beta j} \dot{u}_{\beta j} + K_{\alpha \beta \gamma j} u_{\beta j} u_{\gamma i} + H_{\alpha i \lambda} P_{\lambda} + S_{\alpha i \beta j} u_{\beta j} = 0 \quad \dots (18)$$

$$H_{\alpha i \lambda} u_{\alpha i} = 0 \quad \dots (19)$$

where

$$M_{\alpha i \beta j} = \int_{\mathbf{V}} \rho (\Phi_{\alpha} \Phi_{\beta}) \delta_{ij} dV$$

$$K_{\alpha \beta \gamma j} = \int_{\mathbf{V}} \rho (\Phi_{\alpha} \Phi_{\beta} \Phi_{\gamma j}) dV$$

$$H_{\alpha i \lambda} = - \int_{\mathbf{V}} (\Phi_{\alpha i} \Psi_{\lambda}) dV$$

$$S_{\alpha i \beta j} = \int_{\mathbf{V}} \mu_{eff} (\Phi_{\alpha k} \Phi_{\beta k}) \delta_{ij} dV + \int_{\mathbf{V}} \mu (\Phi_{\alpha i} \Phi_{\beta j}) dV = 0$$

And superposed dot denotes partial differentiation with respect to time (t). The conventional finite element superposition procedure gives the final equation system for the whole flow field in the following form.

$$M_{\alpha \beta} \dot{v}_{\beta} + K_{\alpha \beta \gamma} v_{\beta} v_{\gamma} + H_{\alpha \lambda} q_{\lambda} + S_{\alpha \beta} v_{\beta} = 0 \quad \dots (20)$$

$$H_{\alpha \lambda} v_{\alpha} = 0 \quad \dots (21)$$

where: -

v_α and q_λ denote the velocity and pressure of the whole nodes in the flow field.

By the same method solve the Kinetic energy equation and dissipation equation for the two dimensional flow equations (5 and 6)

The type of the element in the mesh is triangular with (144) element and three nodes for each element Fig.(4).

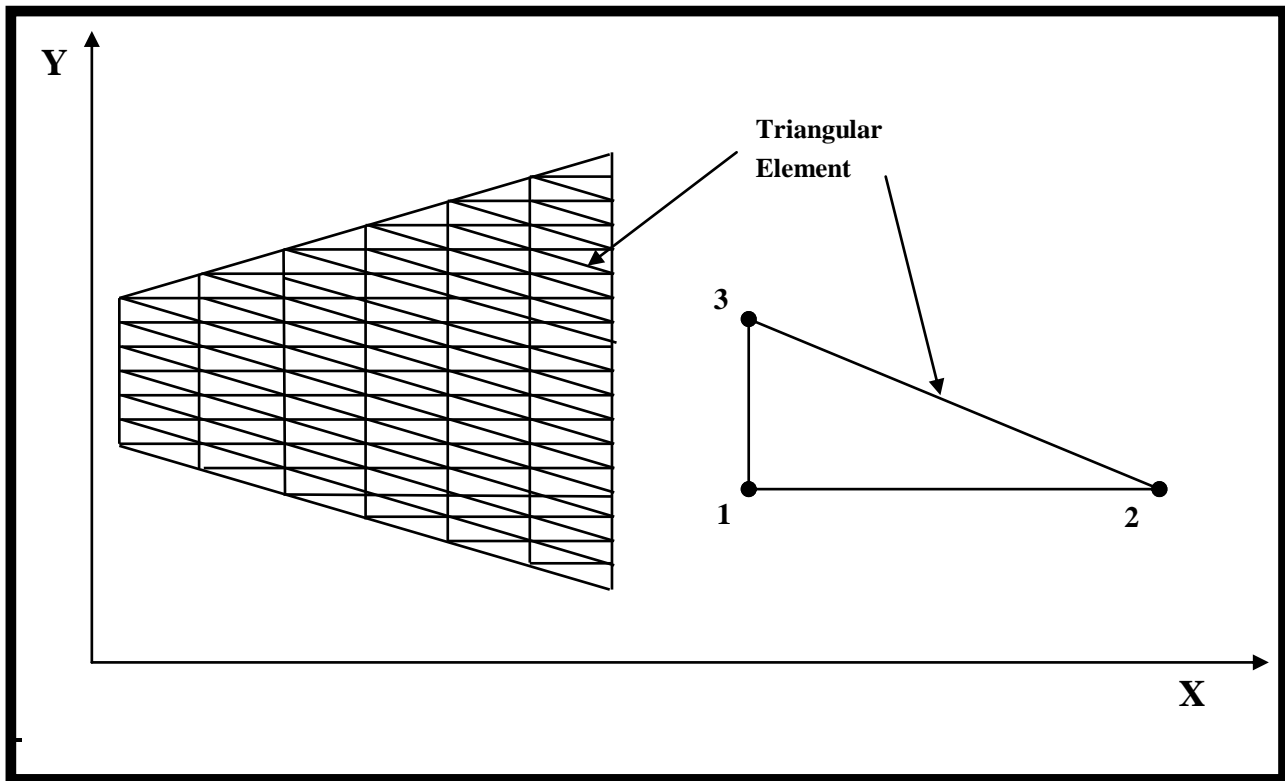


Fig.(4) Natural coordinate triangular element.

5. Computer Program: -

A general purpose computer program Finite element mechanics is to producing the results to be discussed. The program is written and developed in Quick Basic language to solve the two dimensional unsteady flow Ref. [11]. The perturbation method is employed to solve the unsteady flow problem by equations (20 and 21). Assume that the term Ω_α can be expanded into Taylor series in small perturbation parameter (ϵ) as follows.

$$\Omega_\alpha = \Omega_\alpha^0 + \epsilon \Omega_\alpha^1 + \epsilon^2 \Omega_\alpha^2 \quad \dots (22)$$

Expanding velocity v_β and pressure q_λ as:

$$v_\beta = v_\beta^0 + \epsilon v_\beta^1 + \epsilon^2 v_\beta^2 \quad \dots (23)$$

$$q_\beta = q_\beta^0 + \epsilon q_\beta^1 + \epsilon^2 q_\beta^2 \quad \dots (24)$$

Introducing equations (22, 23 and 24) into equations (20 and 21) and equating the coefficients of the same order terms in (ϵ) lead to the following simultaneous equation system :

For the nth order

$$M_{\alpha\beta} v_{\beta}^{\bullet n} + K_{\alpha\beta\gamma} v_{\beta}^n v_{\gamma}^n + H_{\alpha\lambda} q_{\lambda}^n + S_{\alpha\beta} v_{\beta}^n = 0 \quad \dots (25)$$

$$H_{\alpha\lambda} v_{\alpha}^n = 0 \quad \dots (26)$$

Replace the differential with respect to time t by the difference with respect to the short time increment Δt as:

$$v_{\beta}^{\bullet n} = \frac{v_{\beta}^n - v_{\beta}^n(0)}{\Delta t} \quad \dots (27)$$

Where $v_{\beta}^n(0)$ denotes the initial value of the velocity increment for short time increment Δt .

Introducing (27) in (26) get the matrix and solve this matrix by Newton-Raphson method to get on velocity component and pressure at all nodes.

6. Results and Discussion

Several models were taken for different angles (θ), area ratios (AR) and the ratio length/width (L/W_1), the models taken are in table below:

| Model No. | AR | L1/W1 | L2/W1 | L3/W1 | L4/W1 | θ_1 | θ_2 | θ_3 | θ_4 |
|-----------|-----|-------|-------|-------|-------|------------|------------|------------|------------|
| 1 | 1.4 | 3 | 4 | 5 | 6 | 7.63° | 5.73° | 4.58° | 3.82° |
| 2 | 1.6 | 3 | 4 | 5 | 6 | 11.42° | 8.58° | 6.87° | 5.73° |
| 3 | 1.8 | 3 | 4 | 5 | 6 | 15.2° | 11.42° | 9.15° | 7.63° |
| 4 | 2 | 3 | 4 | 5 | 6 | 18.9° | 14.25° | 11.42° | 9.53° |
| 5 | 3 | 3 | 4 | 5 | 6 | 36.86° | 28.07° | 22.62° | 18.92° |
| 6 | 4 | 3 | 4 | 5 | 6 | 53.13° | 41.11° | 33.4° | 28.07° |

Fig.(5) Presented the velocity component at x-direction for path (1). The velocity decreases with increase (X/L) because of increased in divergent angle for the same angle and the velocity increases with decreased angle for the same (X/L).

Fig.(6) Shows the velocity component at y-direction along the diffuser for different angles for path(1) and area ratio (1.4). The velocity decreases along the diffuser for the same angle due to increase in divergent duct. And the velocity increases with decreased the diffuser angle for the distance between (0.1-0.5) and then no effect with increase or decrease angle.

Fig. (7) Presents the pressure recovery coefficient, distribution along the diffuser for path (1). The pressure recovery coefficient increases with the increased distance for the same angle due to the increase in the static pressure because of the decreasing velocity (diffusion process). Pressure recovery coefficient decreases with the increased angle due to the increased absolute velocity and the decreased static pressure and it began from negative value near the wall due to high velocity at

inlet.

Fig.(8) Shows the velocity component at x-direction with area ratio, for path (1) and different (L/W1) The velocity component decreases with increase area ratio for the same (X/L) due to increase in the divergent angle . And the velocity component increase with increase (X/L) for the same area ratio specially when the area ratio above (2).

Fig. (9) Presented the velocity component at y-direction with variable area ratio for path (1) and different (X/L). The velocity component increased slowly with increased area ratio due to increased in divergent angle for the same (X/L). And velocity component decreased with increased (X/L).

Fig.(10) Shows the pressure recovery factor with different area ratio. The pressure recovery factor increased with increased area ratio at the same (X/L) due to increased in divergent angle. And it increased with increased (X/L) at the same area ratio due to increased in angle.

Fig. (11) Shows area ratio with divergent angle (29) for Path (1) and different (X/L). The area ratio increased with increased divergent angle for the same (X/L). And area ratio increased with increased (X/L).

Fig. (12) Present velocity component at x-direction with area ratio for three paths (1, 2 and 3) and for (X/L =3). The velocity component decreased with increased area ratio for the same path. And the velocity component decreased with increased distance from the wall at the same area ratio.

Fig. (13) Fig. (12) Present velocity component at y-direction with area ratio for three paths (1, 2 and 3) and for (X/L =3). The velocity component increased with increased area ratio for the paths (1and 2) and then decreased due to increased in divergent angle. And the velocity component approaches to constant and equal zero for path (3) due to increased distance from the wall and increased velocity component at x-direction.

A comparison between the numerical results from the present mathematical model with other workers analyses was made. Fig. (14), Fig. (15) and Fig. (16) Shows a comparison between the results obtained with that published by Riyadh [1].

Fig. (14) Shows the velocity component ratio at y-direction for diffuser for AR=2, L/W1=6 and path (1). Noted that it have different between the present model (unsteady) and Riyadh [1] (steady) due to effect of an unsteady term ($\frac{\partial}{\partial t}$).

Fig. (15) Present the effect of pressure recovery coefficient across the diffuser for AR=2, L/W1=6 and path (1). It has been found the effect of pressure recovery in steady state is smaller than unsteady state.

Fig. (16) Shows the velocity ratio for AR=2, L/W1=6 and path (1). The velocity ratio decreased with increased distance due to increased in divergent angle but when unsteady state, the velocity decreased less than steady state due to effect the term of unsteady.

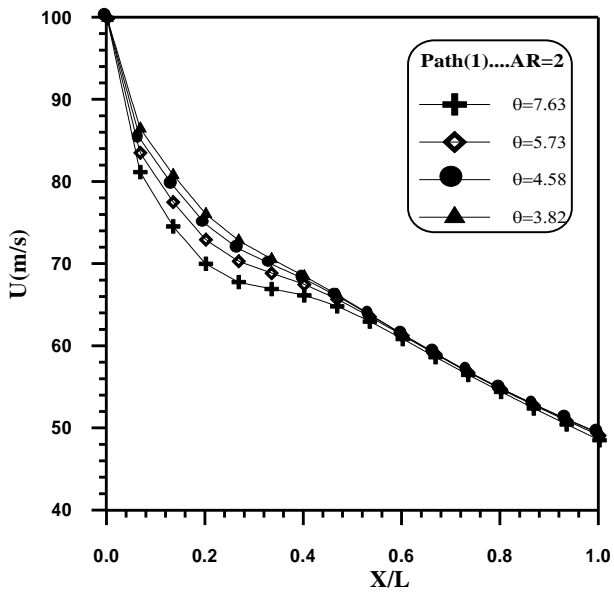


Fig.(5). The velocity component at x-direction for diffuser for path (1).

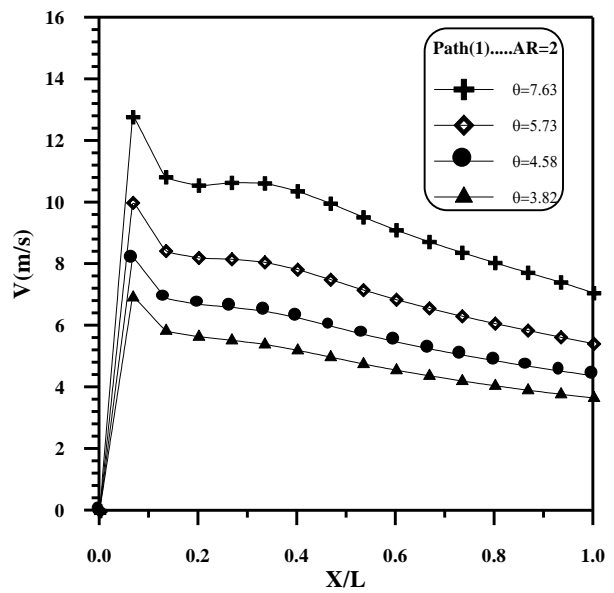


Fig.(6). The velocity component at y-direction for diffuser for path (1).

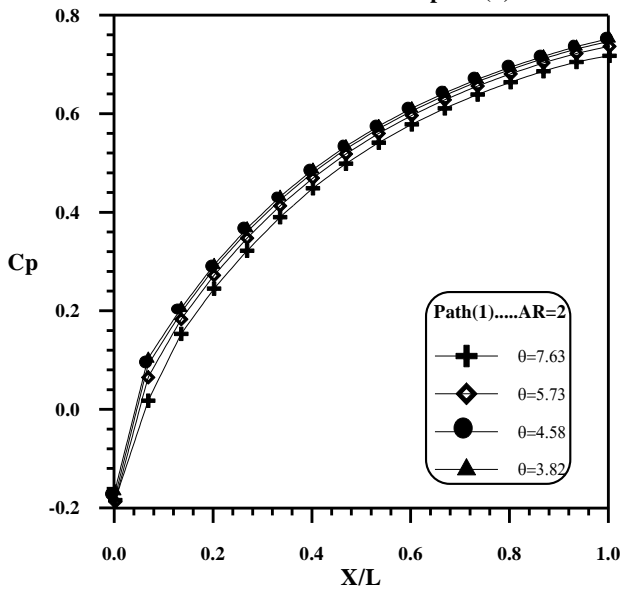


Fig.(7) Effect of pressure recovery coefficient across diffuser for path(1).

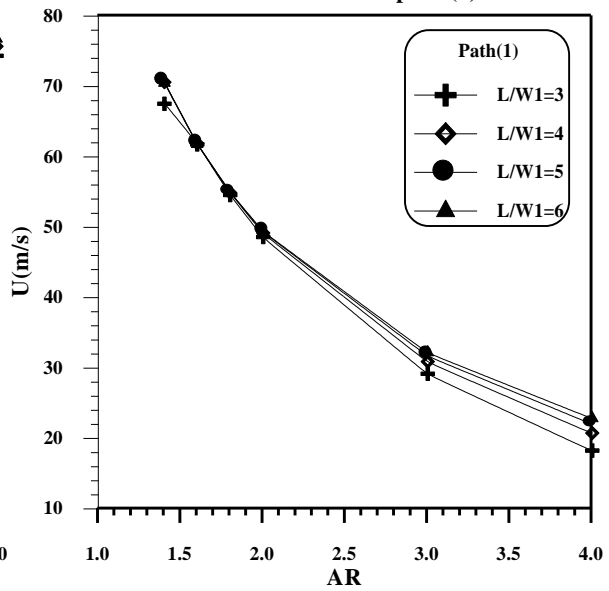


Fig.(8) Effect of velocity component at x-direction for variable area ratio for path(1).

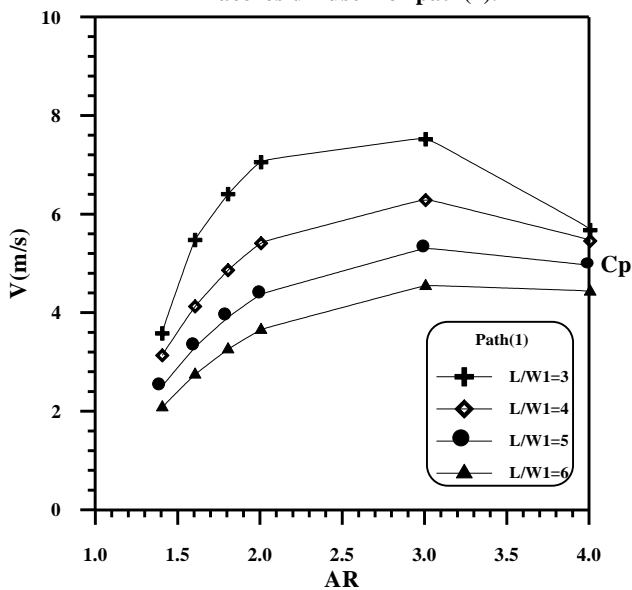


Fig.(9) Effect of velocity component at y-direction for variable area ratio for path(1).

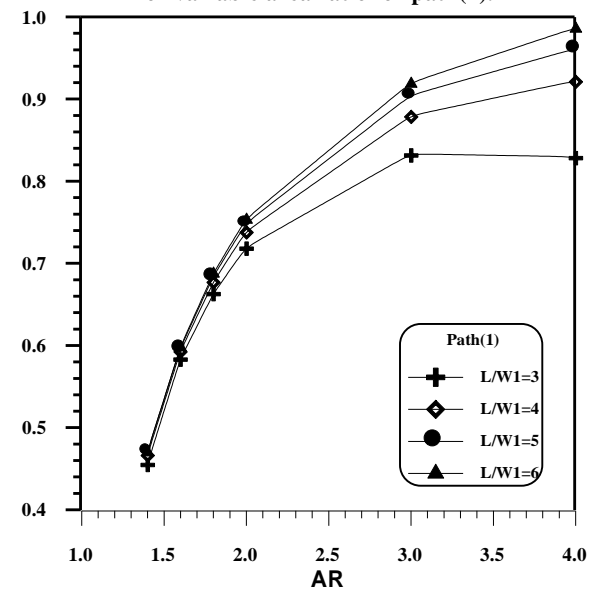


Fig.(10) Effect of pressure recovery coefficient for variable area ratio for path(1).

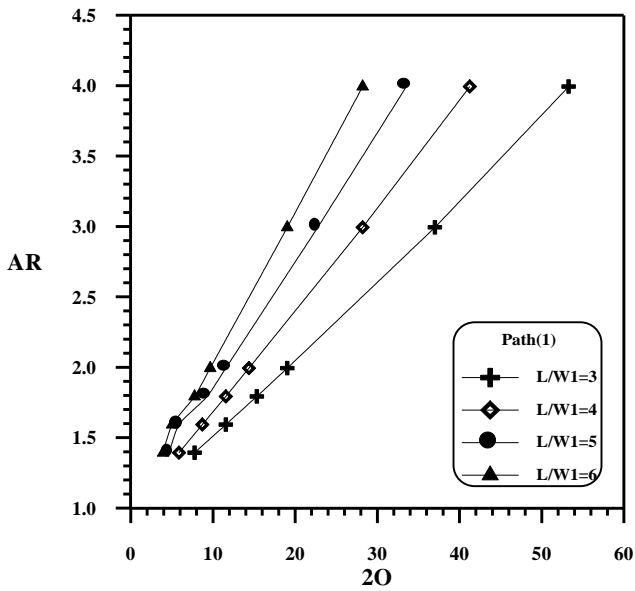


Fig.(11) Effect of area ratio for variable divergent angle of diffuser for path(1).

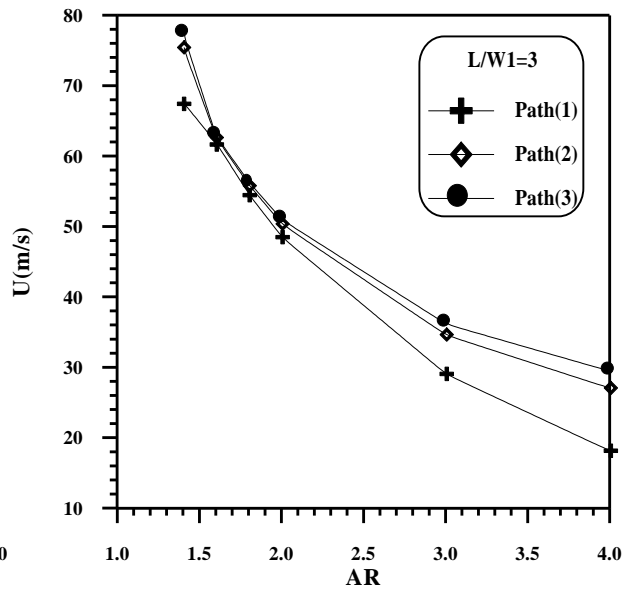


Fig.(12) Effect of velocity component at x-direction for variable area ratio and variable paths.

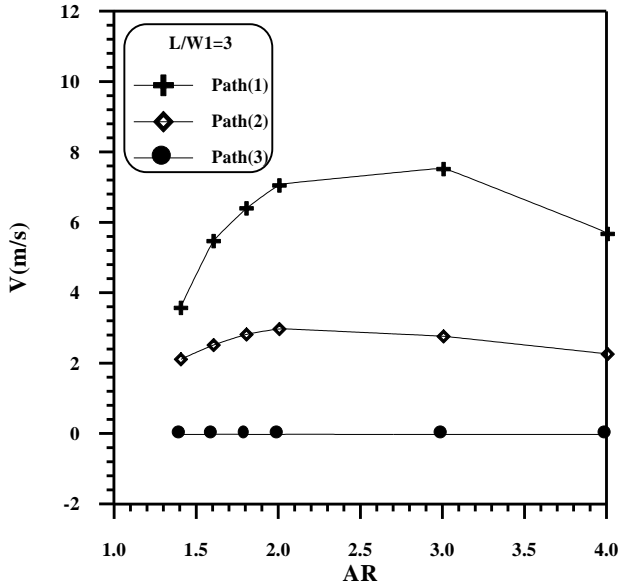


Fig.(13) Effect of velocity component at y-direction for variable area ratio and variable paths.

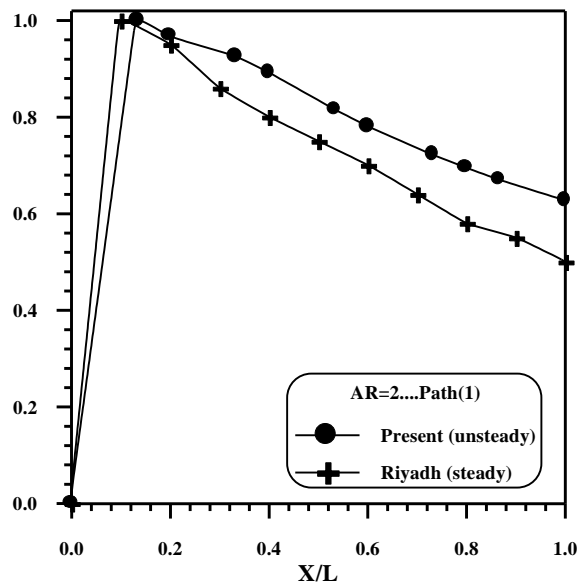


Fig.(14) The velocity component at y-direction for two-dimensional diffuser for path (1).

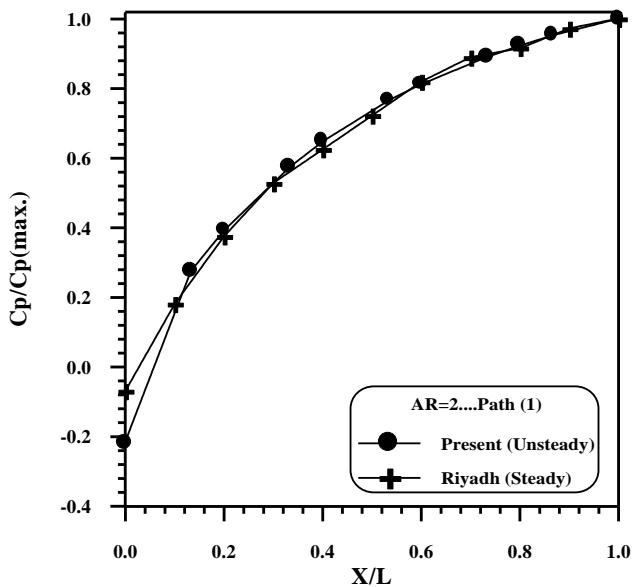


Fig.(15) Effect of pressure recovery coefficient across diffuser for path(1).

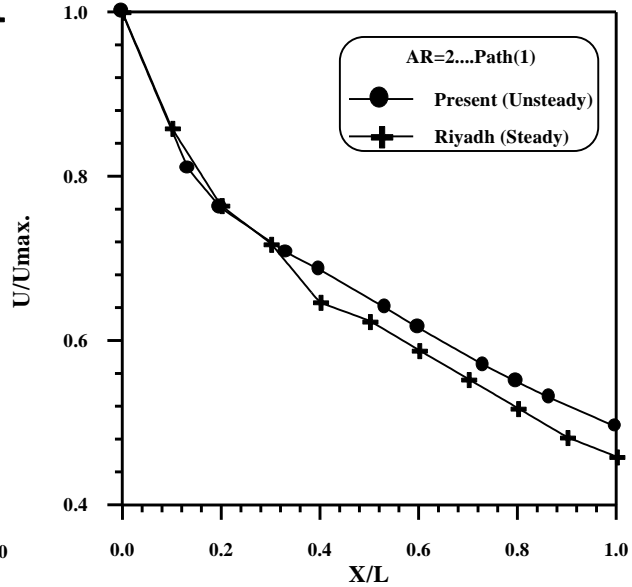


Fig.(16) The velocity component at x-direction for two-dimensional diffuser for path (1).

7. Conclusion

This paper has dealt with a finite element method to analyze unsteady flows of viscous fluid in two dimension of diffuser. Discretization procedure is based on Galerkin approach.. The following conclusion can be made: -

1. From studying the results of analysis of flow throw the diffuser for several models, the geometry data for optimum design found are:
 $AR=2$, $L/W_1=6$ and $\theta = 9.53^\circ$
2. This model gives a pressure recovery coefficient (CP) equal to (0.75) and low velocity component (V) with respect with other models and lows ratio OF (L/W1) with other models. This agrees well with that published by reference [1, 2, and 3].
- 4- Pressure recovery coefficient increase with increase the angle of divergence of diffuser wall and increase in static pressure with decreased in average velocity.

Nomenclature

C_1, C_2, C_μ :- Constant of turbulence.

K:-kinetic energy of turbulence.

ℓ :-Length scale of turbulence.(m)

P_1 :-Inlet static pressure. (N/m²)

P_2 :-Exit static pressure. (N/m²)

C_p :-Pressure recovery coefficient.

L:-Length of diffuser.

ν :-Kinematics viscosity. (m²/s)

u :- velocity component. (m/s)

t :-Time (sec.)

θ :-Divergent angle.(degree)

Ω :-Area of element. (m²)

$\alpha, \lambda, \beta, \gamma$:-The global node number.

σ :-Stress tensor.

W_1 and W_2 :-Inlet exit diffuser width between diverging wall. (m)

b :-distance between parallel walls of a diffuser. (m)

α_{4SS} :- Diffuser vane suction side angle (Fig. 1)

r_2, r_4 :- Radius of impeller.

μ_t :-Laminar viscosity. (kg/m.s)

μ_t :- Turbulent viscosity. (kg/m.s)

ε :-Dissipation rate of turbulence.

μ_{eff} :-Effective viscosity. (kg/m.s)

σ_k :- Turbulence Prandtl number for k-equation

σ_ε :- Turbulence Prandtl number for ε -equation

R:-Radial component.

V_1 =Absolute velocity

C_d =coefficient equal to unity without losses.

X:-axial distance. (m)

ρ :-Density. (Kg/m³)

τ :-Shear stress. (N/m²)

i, j :-Tensor notation subscripts.

AR: area ratio.

REFERENCES

- [1] Riyadh S. Al-Turhee, "**Performance Prediction of Centrifugal Flow Compressor**", M.Sc. thesis, Engineering College, University of Babylon, 2001.
- [2] K. Eisele, A. Öngören,, P. Holbein, and M.V. Casey "**Benchmark for measurements in a planar diffuser with a high inlet turbulence level**" Institute of Hydraulic Machines and Fluid Mechanics Lausanne, Switzerland,2003.
- [3] Kai U. Ziegler¹, Heinz E. Gallus and Reinhard Niehuis, " **A Study on Impeller-Diffuser Interaction: Part 1-Interaction on the Performance** ", No. GT-2002- 0381Proceedings of ASME TURBOEXPO, 2002.
- [4] [8] Adkins, R.C., "**A Short Diffuser with Low Pressure Loss**", Journal of Fluids Engineering, PP. 297-302, Sep. 1975
- [5] Munir Al-Mudhafar, "**Investigation of the performance of a two dimensional diffuser in non-uniform flow**", Ph.D. Thesis. The Hatfield polytechnic school of Engineering, Division of Mechanical & Aeronautical Engineering, 1983.
- [6] Reneah, L.R., Johnston, J.P. and KLINE, S.J., "**Performance and design of straight two-dimensional diffuser**", Journal of Basic Engineering, ASME., March, 1967, PP. 141-150.
- [7] Stow, P., Hirsch, Ch. and Ucer, A.S., "**Thermodynamics and fluid mechanics of turbomachinery**", Vol. II, Martinus Nijhoff publishers, PP. 829-885, 1985.
- [8] Norberto Nigro, Mario Storti and Angel Zanotti, "**Numerical aspects of k-ε Turbulence Modeling using a Finite Element Incompressible Navier-Stokes Formulation**", International Center for Computational Methods in Engineering (CIMEC) INTEC-Universidad Nacional del Litoral-CONICET, G'uemes 3450, 2003
- [9] Garthing, D.K. and Becker, E.B., "**Finite element analysis of viscous incompressible flow**"; Computer method in applied Mechanics and Engineering, 8, PP. 51-60, 1976.
- [10] Ramatalla, M.A.F., "**Computation of three-dimensional flow through turbo machines**", Ph.D. Thesis, Department of Mechanical Engineering the University of Manchester, Institute of Science and technology, 1980.
- [11] Chung, T.J., "**Finite Element Analysis in Fluid Dynamics**", Mc Graw-Hill Company, 1978
- [12]Schamber, D.R. and Larock, B.E., "**Computational aspects of Modeling Turbulent Flow by Finite Elements**", University of California, 1978.